

Evaluation of retinal and choroidal changes in patients with Alzheimer's type dementia using optical coherence tomography angiography

Zebing Li

Shanghai Jiao Tong University Medical School Affiliated Ruijin Hospital

Zhongjing Lin

Shanghai Jiao Tong University Medical School Affiliated Ruijin Hospital

Na Li

Shanghai Jiao Tong University Medical School Affiliated Ruijin Hospital

Huan Yu

Shanghai Jiao Tong University Medical School Affiliated Ruijin Hospital

Yanlin Wu

Shanghai Jiao Tong University Medical School Affiliated Ruijin Hospital

Xi Shen (✉ carl_shen2005@126.com)

<https://orcid.org/0000-0001-9669-6521>

Research article

Keywords: Optical coherence tomography angiography, Alzheimer's type dementia, Mini-mental State Examination, Montreal cognitive assessment scale, RETeval system, flash ERG

Posted Date: December 31st, 2019

DOI: <https://doi.org/10.21203/rs.2.19762/v1>

License: © ⓘ This work is licensed under a Creative Commons Attribution 4.0 International License.

[Read Full License](#)

Abstract

Purpose To evaluate the changes in fundus parameters in patients with Alzheimer's type dementia (ATD) using optical coherence tomography angiography (OCTA), to record flash electroretinograms using the RETeval system and to explore changes in retinal function.

Methods Twenty-nine patients with ATD and 26 age-matched normal subjects were enrolled. All subjects underwent OCTA scans to analyse the superficial retinal vessel parameters in the macular area, including the vascular length density, the vascular width density and the area of foveal avascular zone (FAZ), as well as the choroidal thickness. The differences between the patients with ATD and the normal control group were compared and explored the relevant factors affecting vessel parameters. We also recorded the flash electroretinograms (ERG) using the RETeval system and intended to explore changes in retinal function by analysing the ERG image amplitude in patients with ATD.

Results The vessel parameters and average choroid thickness in the macular area of the ATD group was less than the control group, The FAZ area was statistically significantly enlarged in the ATD group. These parameters were correlated with the Mini-Mental State Examination (MMSE) score and the Montreal Cognitive Assessment (MoCA).

Conclusions Patients with Alzheimer's type dementia exhibit decreases in the parameters associated with fundus. In addition, these indicators significantly correlated with the MMSE score and the MoCA score. OCTA may be an adjunct tool with strong potential to track changes in the diagnosis and monitoring the progression of the disease.

1. Introduction

Alzheimer's type dementia (ATD) is the most common type of dementia and accounts for 60–70% of all causes of dementia. ATD is a progressive neurodegenerative disease that usually manifests as irreversible impairments in cognitive function and behaviour. Characteristic pathological changes include brain atrophy, tangles, loss of neurons in the brain tissue and deposition of extracellular amyloid protein [1]. The increase in the ageing population in society is attributed to the continuous increase in the standard of living and development of medical technology; thus, the incidence of ATD inevitably shows an increasing trend. Therefore, basic and clinical studies of ATD have gradually begun to attract attention from researchers. Currently, the clinical diagnosis of ATD mainly relies on the patient's complaint, Mini-Mental State Examination (MMSE) score, Montreal Cognitive Assessment (MoCA) score, magnetic resonance imaging (MRI) and other imaging examinations designed to assess the intracranial atrophy of the brain tissue. In recent years, an increasing number of ophthalmologists have observed symptoms, such as decreased resolution and reduced contrast sensitivity in visual function in many patients with ATD [2–4]. Changes in the fundus of the retina in patients with ATD have become the focus of research in recent years. Many experts and scholars are eager to determine whether these studies will provide new insights and perspectives for the early clinical diagnosis and prevention of ATD.

Based on the homology of the retina and the brain derived from neural tube development, pathologically speaking, characteristic A β amyloid deposits in the central nervous system have also been found in the retinas of both patients with ATD and ATD transgenic mouse models. Retinal A β deposits and imaging techniques are also being used for the early detection of potential biomarkers in the retinas of patients with ATD [5–6]. In addition to the A β deposits, abnormal hyperphosphorylation of the Tau protein has been detected in the brain tissue of the ATD transgenic mouse model, and the hyperphosphorylation of the Tau protein is also observed in the retina of the mouse. The levels of this protein in the posterior region are greater than in the peripheral region [7]. These pathological evidence implies the homology of retina and brain tissue. ATD may not only cause lesions in the brain tissue but also in the retina. Therefore, many experts and scholars at home and abroad have also invested extensive research efforts in this area with the aim of conducting early screening of the retina through a non-invasive examination to prevent AD and exploring whether these changes will play a certain guiding role in the treatment.

The most common vessel problems in the brains of patients with ATD include impaired A β clearance, impairments in the blood-brain barrier, decreased vessel density, decreased vessel diameter and decreased blood flow [8]. Additional studies are needed to determine whether similar changes will occur in the retina. In recent years, the introduction of optical coherence tomography angiography (OCTA) technology and its gradual promotion as a non-invasive and rapid fundus retinal vessel examination technology has gradually been welcomed by clinicians. Our study aims to discover changes in retinal vessels and the function of the fundus in patients with ATD using OCTA and flash ERG. These findings may contribute to the early diagnosis, prevention, and follow-up of ATD.

2. Materials And Methods

2.1 Research Subjects

The study was conducted at Ruijin Hospital affiliated with Shanghai Jiao Tong University School of Medicine, and it was approved by the Ethics Committee of Ruijin Hospital affiliated with Shanghai Jiaotong University School of Medicine and conformed to the Declaration of Helsinki. Patients with neurological memory disorders were recruited at the clinic from December 2017 to January 2019. Untreated patients with ATD were diagnosed by experienced senior neurologists, while local healthy residents were recruited as the normal control group. Each subject carefully read the informed consent form and signed it to indicate his/her willingness to participate in the study prior to recruitment.

The participants with ATD were diagnosed according to the criteria for dementia established in the 4th edition of the Diagnostic and Statistical Manual of Mental Disorders. All participants were subjected to an analysis of complete routine blood biochemical parameters, including measures of thyroid function, vitamin B12 levels and folic acid levels; MMSE and MoCA scores; and MRI and EEG. Additionally, the spherical mirror was between +3.0D and -6.0D, and the cylinder was between \pm 3.0D for all subjects at enrolment. The slit lamp examination indicated that the anterior segment of the eye was normal and the signal strength of the OCTA image must be greater than 6. The following exclusion criteria were used:

severe cardiovascular disease, liver and kidney dysfunction, respiratory diseases, intracranial lesions and blood diseases, changes in the fundus observed in patients with anterior segment diseases (such as keratitis, anterior chamber opacity and haemorrhaging, and severe cataracts), fundus diseases (such as fundus haemorrhaging, macular degeneration, diabetic retinopathy, and uveitis), other eye diseases that affect vision (such as colour blindness, retinitis pigmentosa, and optic neuritis), a history of eye surgery, history of trauma, and history of exposure to lasers.

2.2 Inspection Method

2.2.1 Ophthalmic examination

All subjects underwent a series of detailed eye examinations, including the best corrected visual acuity measured using the international standard eye chart, the anterior segment examination using the slit lamp, the diopter (RK-F1 from Nedek, Japan), and the intraocular pressure (IOP) (Goldmann flattening tonometer) before the OCTA test. The central corneal thickness (CCT) and axial length (IOL-Master of Zeiss, Germany) and chamber angle were examined using a gonioscope, and direct and indirect ophthalmoscopy were used to examine the fundus. Although both eyes of all subjects were examined, if both eyes met the enrolment conditions, one eye was randomly selected for inclusion in the study to avoid binocular interactions.

2.2.2 Optical Coherence Tomography angiography (OCTA)

All OCTA measurements were performed by the same physician skilled in the technique. Inspections were performed using a Zeiss light coherence tomography scanner (Carl Zeiss Meditec, Germany). Compound tropicamide eye drops were administered to both eyes to dilate the pupils. After at least 30 minutes, the physician ensured that the pupil sphincter of the tested eye was relaxed and pupil dilation was complete. Angiography 6×6 mm, angiography 3×3 mm and EDI modes were chosen. The signal strength of all OCT images should be greater than 6.

The angiography 6×6 mm model was chosen and centred on the macular area through the 1, 3, 6 mm ETDRS (Figure 1) to partition the macular area F (foveolar subfield), IT (inner temporal subfield), II (inner inferior subfield), IN (inner nasal subfield), IS (inner superior subfield), OT (outer temporal subfield), OI (outer inferior subfield), ON (outer nasal subfield), and OS (outer superior subfield). Figure 2A shows the superficial retina from the internal limiting membrane (ILM) to the inner plexiform layer (IPL), which was examined to collect the superficial retina blood flow signals and analyse the overall vessel length density and vessel width density. The vessel length density calculates the value of the vessel length density in the region by depicting the linear length of blood vessels to more accurately observe the degree of perfusion of microvessels. The width density reflects the diameter of blood vessels and the degree of perfusion of blood flow in blood vessels by depicting the diameter and width of blood vessels and calculating the density of blood vessel coverage in the region. The angiography 3×3 mm model was used to measure the area of the foveal avascular zone (FAZ) (Figure 2B-D).

In EDI mode, the scanning line of 6 mm was used to scan the 0° horizontal line and the 90° vertical line around the macular area. The site of the macular area that was measured is the central concave and the upper, lower, nasal and temporal sides, and the distances from the fovea were 500 µm, 1000 µm, 1500 µm and 2000 µm, respectively (Figure 3). Self-designed measurement software (Figure 4) was used to measure the vertical thickness of the choroid at the corresponding position. The inner boundary of the choroid is the retinal pigment epithelial layer, while the outer boundary of the choroid is the inner sclera [9] (Figure 4), and the mean choroidal thickness was calculated.

2.2.3 RETeval system records of flash electroretinograms (ERGs)

The recording system consisted of a hand-held stimulator, recording device and analysis device (weight 232 g; Figure 5A-a). A docking station charges the machine and uploads the recorded results to the computer (Figure 5A-b), a soft eye mask touches the bony area around the eye (Figure 5A-c), and a disposable skin electrode array receives electrical signals (Figure 5A-d). Flash stimuli are derived from the bottom of a 60 mm diameter dome-shaped structure. White light stimuli were administered by trichromatic LEDs (red, 622 nm; green, 530 nm; blue, 470 nm; CLV6A-FKB; Cree, Inc., Durham, NC, USA). The frequency of the scintillation stimulus was 28.306 Hz and the pulse duration was less than 1 millisecond. The centre of the dome features a red gaze point (Fig. 5B, red arrow), and the subject looks at the point during the collection of ERG data. The acquisition process is shown in Figure 5C. A special skin electrode array (LKC Technologies, Inc.) was placed on a rim of 2 mm from the inferior temporal margin (Fig. 5A-d and 5D). The electrode array comprises three electrodes, a positive electrode, a negative electrode and a ground electrode, with a tape attached to each (Fig. 5E). The new handheld RETeval recording ERG system reduces the damage to the cornea and ocular surface caused by rigid corneal contact electrodes and improves the comfort level of subjects compared with traditional retinal galvanogram recording devices. The collection of retinal electroretinograms from subjects with partial poor corneal epithelial conditions and partial poor compliance (children) was thoroughly addressed. We chose the international general ISCEV five-step protocol that starts with dark adaptation. Subjects first underwent dark adaptation in a dark environment for 30 minutes. The second step was mainly used to collect the mixed reaction data from cone and rod cells (flash: 3.0 cd·s/m², chromaticity (0.33, 0.33) (0.1 Hz) backlight: 0.0 cd/m²). Many waveforms are present in the response wave, the most important of which are the first two waveforms: a negative waveform (a wave, measuring the distance from the baseline to the trough) followed by a positive waveform (b wave, measuring the distance from the baseline to the crest). The a wave reflects the activity of photoreceptor cells, and its amplitude mainly reflects the function of rod cells. The b wave reflects the function of the inner layer of the retina (the bipolar cells of rods and cones and Muller cells). The amplitude (the distance from peak to trough) was used as the main reference index to evaluate the responses of cones, rods and Muller cells, and to explore the difference in ocular visual function between patients with ATD and the normal control group.

2.2.4 Statistics

SPSS 20.0 software was used for the statistical analysis of all data. The measured data are reported as means \pm standard deviations, and the Kolmogorov-Smirnov method confirmed that all data from each group were normally distributed. The independent sample t-test was used to compare the basic information (age, intraocular pressure, ocular axis, the central corneal thickness, MMSE, MoCA, etc.), vessel length density, vessel width density, FAZ area and choroid thickness parameters between the ATD and normal control groups. The single factor regression analysis was used to determine the correlations between the parameters and basic data. Since MMSE and MoCA scores play an important role in ATD staging, the correlations between the scores for each assessment and various vessel parameters were further evaluated after correcting for other basic factors using a partial correlation analysis. In addition, we performed a multivariate regression analysis to explore the relevant factors influencing the vessel density, blood perfusion, FAZ area and choroid thickness. $P < 0.05$ was considered statistically significant.

3. Results

3.1 Comparison of basic data

The results are presented in Table 1. Twenty-nine patients with ATD were enrolled, including 15 males (51.7%) and 14 females (48.3%). Twenty-six normal healthy individuals were recruited at the same time, including 10 males (38.5%) and 16 females (61.5%). All subjects enrolled in the study were Asian. No significant differences were identified in gender and eye distribution between the two groups ($\chi^2=0.973$, $P=0.324$ and $\chi^2=0.010$, $P=0.921$, respectively). Significant differences in mean age, IOP, axial length, and CCT were not observed between the ATD group and the normal control group ($t=-0.738$, $P=0.088$; $t=-0.767$, $P>0.05$; $t=-1.644$, $P>0.05$; and $t=0.809$, $P>0.05$, respectively). Statistically significant differences in MMSE and MoCA scores were observed between the ATD group and the normal control group ($t=7.343$, $P<0.001$ and $t=11.090$, $P<0.001$, respectively).

3.2 Analysis of surface retinal vessel parameters

With the exception of the outer temporal and outer nasal regions, the vessel length density and vessel width density in other regions were significantly different between the two groups (t between 2.152 and 3.982, all $P < 0.05$). Tables 2 and 3 provide a detailed description of the surface retinal blood vessel parameters in different measurement areas.

A regression analysis was performed on all subjects in this study, and the results are presented in Table 4. Similar to the vessel length and width density in some regions, with the exception of the outer temporal and outer nasal regions, the parameters of patients with ATD were lower than the Normal group. The average vessel length density and the average vessel width density from representative regions were selected for the regression analysis. Univariate regression analysis revealed negative correlations between the complete vessel length density in the macular area with age and axial length ($bb=-0.099$, $P=0.027$ and $bb=-0.599$, $P=0.025$, respectively). This parameter was positively correlated with the MMSE and MoCA scores ($bb=0.293$, $P=0.002$ and $bb=0.194$, $P=0.004$, respectively). The complete vessel width

density in the macular area was negatively correlated with age and axial length (bb=-0.002, P=0.034 and bb=-0.017, P=0.013, respectively). It was positively correlated with MMSE and MoCA scores (bb=0.007, P=0.002 and bb=0.005, P=0.004, respectively). Significant correlations with other factors, including IOP and CCT, were not observed (all P>0.05). The independent variables with P<0.1 in the univariate regression analysis were included in the multivariate regression analysis. The results showed that the complete vessel length density in the macular area was negatively correlated with the axial length (bb=-0.527, P=0.034) and significantly positively correlated with the MMSE score (bb=0.275, P=0.002). The complete vessel width density in the macular area was negatively correlated with the axial length (bb=-0.015, P=0.016) and significantly positively correlated with the MMSE score (bb=0.007, P=0.003). After adjusting for age and the MoCA score, the multivariate regression analysis revealed that the MMSE score and axial length were the most significant factors influencing the retinal vessel parameters in the superficial layer of the macular area in the two groups (Figure 6).

3.3 Foveal avascular zone (FAZ) and choroidal thickness (CT)

The average FAZ area in the ATD group was $0.416 \pm 0.11 \text{ mm}^2$ and the value in the normal control group was $0.243 \pm 0.08 \text{ mm}^2$; the difference statistically significant ($t=-6.858$, $P<0.05$). A regression analysis was performed on all subjects in this study, and the results are shown in Table 5. The univariate regression analysis revealed negative correlations between the FAZ area in the macular area and the MMSE and MoCA scores (bb=-0.342, P=0.011 and bb=-0.451, P=0.001, respectively). Significant correlations with other factors, including age, axial length, IOP and CCT, were not observed (all P>0.05). The independent variable with P<0.1 in the univariate regression analysis was included in multivariate regression analysis, and the FAZ area in the macular area was negatively correlated with MoCA score (bb=-0.011, P=0.001). The multivariate regression analysis showed that the MoCA score was the most significant factor affecting the FAZ area in macular area in the two groups after adjusting for the MMSE score.

The average choroidal thickness in the macular area of the ATD group ($203.68 \pm 14.20 \text{ }\mu\text{m}$) was thinner than in the control group ($240.79 \pm 15.08 \text{ }\mu\text{m}$) ($t=9.889$, $P<0.001$). A regression analysis was performed on all subjects in this study, and the results are presented in Table 6. According to the univariate regression analysis, the average choroidal thickness in the macular area was negatively correlated with age (bb=-0.803, P=0.009) and positively correlated with the MMSE and MoCA scores (bb=5.638, P<0.001 and bb=4.053, P<0.001, respectively). Significant correlation with other factors including axial length, intraocular pressure, and central corneal thickness, were not observed (all P>0.05). The independent variable with P<0.1 in the univariate regression analysis was included in the multivariate regression analysis, and the average choroidal thickness in the macular area was negatively correlated with the MoCA score (bb=-0.011, P=0.001). The multivariate regression analysis showed that the MoCA score was the most significant factor affecting the average choroidal thickness of the macular area in the two groups after adjusting for age and the MMSE score.

3.4 Differences in flash electroretinograms (ERGs)

Flash electroretinograms were recorded with the RETeval system for all enrolled subjects. The average amplitude of the ATD group ($130.967 \pm 21.73 \mu\text{V}$) was smaller than the normal control group ($149.540 \pm 30.90 \mu\text{V}$) ($t = -2.199$, $P = 0.034$). Based on the flash ERGs, patients with ATD have a lower response to the flash in the dark than the normal control group.

4. Discussion

Over time and with the progression of technology, the physiological age of humans is increasing, and neurodegenerative diseases, such as ATD, are attracting increasing attention from the public. The adverse effects of these diseases on the daily lives of the elderly also interfere with the lives of many families. As ATD is a common disease in neurology, pathological changes in intracranial nerves have been identified [1]. The accompanying reduction in the thickness of the retinal neuroepithelial layer of the eyes has gradually become a consensus sign [10–17]. However, few studies have examined parameters related to retina and choroidal blood vessels of patients with ATD; thus, this study was designed in an attempt to explore these parameters.

The most common intracranial vessel changes observed in patients with ATD include impaired self-clearance of the A beta protein, impairments in the blood-brain barrier, decreased vessel density, decreased vessel diameter, and decreased blood flow [18]. These findings provide good insights into the potential changes in the retina and choroid, because the vessels in these structures are homologous to those in the brain. In our study, the detailed vessel distribution parameters near the macular area were precisely analysed using zoning. The blood vessel length density and blood vessel width density in different areas of the macula of patients with ATD were lower than the normal control group, except the outer ring nasal area and outer ring temporal area. The automatic regulation of the human circulation is complex, and many factors ensure a stable local blood supply when vascular density parameters change. The process of autoregulation depends on the local mitogenic response, endothelium-derived substances, local metabolic factors and the autonomic nerves [19]. A decrease in the vascular density might not directly reflect a decrease in the retinal blood supply in patients with ATD, but we observed changes in the retinal microcirculation of patients with ATD by performing a comparative analysis, which provided support for the clinical prospect of the OCTA-assisted diagnosis of ATD.

The retinal vessel system including radial capillary network near nipples, shallow vessel plexus and three parts of the deep vessel plexus [20], the deep shallow vessel plexus and vessel plexus near the centre concave and macular area of avascular area, called the foveal avascular zone (FAZ) [21]. In previous studies, the FAZ area was enlarged in patients with diabetic retinopathy and macular branch vein occlusion, according to an FFA examination. Moreover, the FAZ is extremely susceptible to changes in local blood supply, and an increase in the FAZ area is a sign of ischaemia. Thus, the blood supply of the retina can be measured by observing the changes in the FAZ area [22–23]. In our study, the FAZ area was significantly increased in patients in the ATD group compared with the normal control group. Based on this result, the blood supply of the shallow retina is affected by such diseases as ATD, showing a decreasing trend. The results of this study should be confirmed using colour Doppler imaging (CDI).

After discovering statistically significant differences between the aforementioned indicators, our research began to focus on the relevant influencing factors. Basic data were collected for all subjects, including age, IOP, axial length, CCT, MMSE score, and MoCA score. According to the univariate linear regression analysis, the surface vessel parameters, complete vessel length density and complete vessel width were negatively correlated with age and axial length, and positively correlated with the MMSE and MoCA scores. Age and axial length were the two main factors affecting the surface vessel parameters of the macular area in previous studies [24–27], and these results were consistent with univariate correlation analysis. Therefore, when we explore the effects of diseases such as ATD on retinal blood vessels, the difference in mean values must be considered when determining the effects of confounding factors. After adjusting for age and MoCA scores, the MMSE score was positively correlated with the parameters, and the axial length was negatively correlated with the parameters in the multivariate regression analysis. The MMSE score and axial length were the most significant factors affecting the surface retinal vessel parameters in the macular area. As one of the diagnostic criteria for clinical ATD, the MMSE score can be used as an index of disease progression. We concluded that the severity of ATD disease progression is significantly correlated with surface retinal vessel parameters in the macular area. In the comparative analysis of FAZ and CT, after considering the combined effects of confounding factors, the MoCA score was significantly negatively correlated with FAZ. MoCA is also one of the diagnostic criteria for ATD, and a high score also indicates an increasing severity of the disease. Therefore, we postulate that the degree of progression of ATD disease is more serious, and the distribution of the vasculature to the surface of the retina in the macular area will gradually decrease.

The Mini-Mental State Examination (MMSE) score comprehensively, accurately and quickly reflect the subject's mental state and level of cognitive impairment. The MMSE score provides scientific evidence for a clinical psychology diagnosis, treatment and neuropsychological research. This score is widely used at home and abroad, and it is the preferred scale for dementia screens. However, the scoring system also has certain limitations. The MMSE scoring system covers fewer cognitive domains, and the two cognitive domains of orientation and language ability are assessed in a relatively large proportion of questions. The proportion of questions assessing other cognitive domains is small, and the scores for each cognitive domain differ. Memory testing is relatively straightforward and is not sensitive to screens for impairments in individual cognitive domains (such as memory and executive function). For patients with higher education levels, the scale is in the normal range because the assessment is too simple, which easily conceals the cognitive impairment of patients [28–33]. The Montreal Cognitive Assessment (MoCA) score is an assessment tool used to quickly screen for cognitive dysfunction. A screen for mild cognitive impairment (such as amnesic cognitive impairment) and suspected dementia in a single cognitive domain is more sensitive. The cognitive domain is more extensive and comprehensive, the score distribution is more reasonable. The scores for visual space and executive function are improved, the memory test is more reasonable, the number and difficulty of words are increased, and the time of delayed recall is prolonged. MoCA reflects the true state of the patient's memory. However, the score requires patients to have a certain level of literacy and ability to cooperate, and no study with a large sample size either at home or abroad has screened for cognitive impairment using MoCA. Thus, a

recognized threshold for screening for dementia and mild cognitive impairment is not available [34–37]. Although the two scoring systems have advantages and disadvantages, experts and scholars at home and abroad indicate that the MoCA score is more sensitive and accurate than the MMSE score [34–37]. In our study, after adjusting for the confounding effects of multiple factors, the MMSE score was significantly associated with the surface retinal vessel parameters in the macular area, while the MoCA score was significantly associated with the area of the fovea in the macular area. As we mentioned above, the FAZ surface is actively affected by changes in local blood supply. Therefore, is the effect on the retinal blood supply caused by changes in the FAZ area more sensitive than changes in the surface retinal blood vessel parameters? In addition, does this difference in sensitivity coincide with the difference in sensitivity between the MoCA and MMSE scores? In-depth investigations of big data will be worthwhile. In addition, the differences in statistical correlations may also provide corresponding recommendations for the current clinical diagnosis of ATD. The combination and complementation of the two scoring systems might provide a better method for AD diagnostic screening.

Since software that automatically divides and measures the choroidal thickness using OCT instruments is not available, most research projects still require the observer to manually draw the inner and outer lines of the choroid and use manual callipers to complete all measurements, which inevitably introduces certain measurement errors. All measurements in this study were performed using a self-designed image measurement software to minimize measurement errors. In our study, the mean choroidal thickness in the macular area of the ATD group was less than the normal group, and the mean difference was statistically significant. After correction, univariate and multivariate regression analyses revealed a positive correlation between the MoCA score and the choroidal thickness in the macular area. The choroidal membrane accounts for 80–90% of the total blood flow to the eye and plays important roles in providing nutrition to outer layer of the retina and maintaining the structure and function of the retina. Amyloid deposits in the choroid, particularly in the choriocapillaris, have been reported in a histopathological study of a patient with primary systemic amyloidosis by Ts'o and Bettman [38]. On the other hand, Roybal et al. [39] retrospectively analysed 4 patients with amyloid-induced chorioretinopathy and reported a thicker hyporeflective choriocapillaris band in the OCT images that was caused by the accumulation of amyloid deposits. Because amyloid deposits are typical pathological manifestations of ATD, researchers have speculated that the degree of progression of ATD is more serious, and the altered blood flow to the outer layer of the retina will increase. The decrease in the choroid thickness may be related to choroid atrophy secondary to amyloid angiopathy. According to several independent studies, patients with ATD present with different types of visual dysfunction, such as decreased colour vision sensitivity and contrast sensitivity defects [40–43]. Both the choroidal circulation and retinal circulation are involved in meeting the metabolic requirements of photoreceptors for oxygen [44]. The retina requires a continuous supply of oxygen. If the intraocular pressure suddenly increases to the average level of systemic arterial pressure, the retinal vessel circulation is interrupted. Vision disappears only in 4–9 seconds [45–46]. In addition, scintillation stimulation increases the retinal vessel diameter and retinal blood flow [47–51]. Under physiological conditions, the retinal blood flow supply is closely related to the normal execution of its function. In our study, a new and convenient RETeval system was used to record flash electroretinograms,

and the amplitude (peak to trough distance) was used as a primary reference to evaluate the response of cones, rods and Müller cells. The retinal response to flash stimuli decreased in patients with ATD. This result is consistent with our hypothesis about the obstruction of choroid blood flow. Although the research in this area is not extensive, our findings provide a potential insight into the relationship between blood supply and visual function of patients with ATD, but further studies are needed in the future.

This research also has some limitations. First, the analysis of vessel parameters was limited to the inner boundary membrane layer and the inner plexus layer; we were unable to obtain the deeper retinal vessel parameters due to the limitations of the analysis software. Second, as a non-invasive technique for measuring choroidal thickness, EDI-OCT has excellent repeatability. However, it only reflects a static structure rather than dynamic changes in blood flow and does not accurately describe the haemodynamic characteristics of the choroid. Therefore, some important information may be lost. Third, some researchers have shown dynamic changes in the choroidal thickness in 24 h [52–54]. Although the imaging data collected from subjects in our study were mainly recorded in the afternoon (14:00–17:00), errors were not able to be completely excluded. Moreover, we manually measured the choroidal thickness at several sites and thus were unable to completely exclude measurement error and local choroidal changes. These limitations are supported by technological innovations that automatically delineate choroidal regions and measure thickness, and we anticipate that more studies of this topic supported by new technologies will be published in the future. Fourth, the data of flash ERGs varied substantially. Conditions permitting, a larger number of subjects will effectively improve the reliability of the data.

In contrast to the traditional ATD diagnostic approach assessing changes in brain and neural function, we examined the changes in the microcirculation of the retina and fundus of patient with ATD, a degenerative disease, using OCTA in the present study. Our selected subjects tended to be patients with early- and middle-stage ATD, and the changes in the microcirculation observed using OCTA may be auxiliary diagnostic criteria for ATD. Using non-interventional methods, ATD screening was conducted at the early stage to achieve the early prevention and administer clinical interventions for ATD. On the other hand, a study assessing the long-term follow-up of patients with ATD using OCTA also has potential for development and may provide a more convenient and intuitive conclusion regarding the effect of treatments on ATD. OCTA has strong prospects for the clinical diagnosis and follow-up of ATD.

5. Conclusions

Compared with normal controls, patients with Alzheimer's type dementia exhibited decreases in the vessel parameters of the surface of retina, an increase in the area of foveal avascular zone, and a decrease in the choroidal thickness. These results suggest changes in microcirculation in patients with Alzheimer's disease. These changes are likely to be related to amyloid deposits caused vascular atrophy or increased blood flow resistance. Moreover, these indicators were significantly correlated with the Mini-Mental State Examination (MMSE) score and the Montreal Cognitive Assessment (MoCA) score. The severity of the disease is involved in the process of changes in the microcirculation of the fundus. The flash ERG showed that people with Alzheimer's disease exhibited a reduced retinal function compared to normal

people. Optical coherence tomography (OCTA) may be an adjunctive diagnostic standard for cognitive disorders and may play important roles in follow-up and evaluating the efficacy of medications.

Declarations

Ethics approval and consent to participate

This research received the ethical approval from Ruijin Hospital, affiliated with Shanghai Jiao Tong University School of Medicine. All procedures were in accordance with the Declaration of Helsinki. All participants signed informed consent forms to participate in the study.

Consent for publication

Written informed consents for publication of the clinical details were obtained from the patients.

Availability of data and materials

All data and materials are fully available in the paper without restriction.

Competing interests

The authors declare that there were no competing interests regarding the publication of this paper.

Funding

None.

Authors' contributions

Conceptualization of the study: ZBL and XS. Data acquisition: ZBL, YLW,NL, HY. Manuscript preparation: ZBL. Revision of manuscript: ZJL and XS. All authors have read and approved the final manuscript.

Acknowledgements

We do not have anyone to acknowledge.

Abbreviations

ATD☒Alzheimer's type dementia

OCTA☒optical coherence tomography angiography

FAZ☒foveal avascular zone

ERG☒electroretinograms

MMSE Mini-Mental State Examination

MoCA Montreal Cognitive Assessment

MRI magnetic resonance imaging

IOP intraocular pressure

CCT central corneal thickness

CT choroidal thickness

References

1. Turner RC, Lucke-Wold B, Robson M, et al. Alzheimer's disease and chronic traumatic encephalopathy: Distinct but possibly overlapping disease entities. *J Brain Inj*. 2016;30(11):1-14. DOI:10.1080/02699052.2016.1193631
2. Gilmore GC, Levy JA. Spatial contrast sensitivity in Alzheimer's disease: a comparison of two methods. *Optom Vis Sci* 1991; 68: 790–794. DOI:10.1097/00006324-199110000-00006
3. Neargarder SA, Stone ER, Cronin-Golomb A, Oross S. The impact of acuity on performance of four clinical measures of contrast sensitivity in Alzheimer's disease. *J Gerontol B Psychol Sci Soc Sci* 2003; 58: 54–P62.
4. Cronin-Golomb A. Vision in Alzheimer's disease. *Gerontologist* 1995; 35: 370–376.
5. Koronyo-Hamaoui M, Koronyo Y, Ljubimov AV, Miller CA, Ko MK, Black KL, et al. Identification of amyloid plaques in retinas from Alzheimer's patients and noninvasive in vivo optical imaging of retinal plaques in a mouse model. *Neuroimage*. 2011;54 Suppl 1:S204–17.
6. Gupta VK, Chitranshi N, Gupta VB, et al. Amyloid β accumulation and inner retinal degenerative changes in Alzheimer's disease transgenic mouse. *Neurosci Lett*. 2016 Jun 3;623:52-6.
7. Lucia Y, Du, Lily Y-L, Chang, Alvaro O, Ardiles. Alzheimer's Disease-Related Protein Expression in the Retina of *Octodon degus*. *PLoS One*. 2015; 10(8)
8. Patton N, Aslam T, MacGillivray J, et al. Retinal vascular image analysis as a potential screening tool for cerebrovascular disease. *J Anat* 2005;206:318–48.
9. Vuong VS, Moisseiev E, Cunefare D, et al. Repeatability of choroidal thickness measurements on enhanced depth imaging OCT using different posterior boundaries. *Am J Ophthalmol*. 2016; 169: 104-112.
10. Cunha LP, Lopes LC, Costa-Cunha LV, Costa CF, Pires LA, Almeida AL, et al. Macular thickness measurements with frequency domain-OCT for quantification of retinal neural loss and its correlation with cognitive impairment in Alzheimer's disease. *PLoS One*. 2016;11:e0153830.
11. Kirbas S, Turkyilmaz K, Anlar O, Tufekci A, Durmus M. Retinal nerve fiber layer thickness in patients with Alzheimer disease. *J Neuroophthalmol*. 2013;33:58–61.

12. Lu Y, Li Z, Zhang X, Ming B, Jia J, Wang R, et al. Retinal nerve fiber layer structure abnormalities in early Alzheimer's disease: evidence in optical coherence tomography. *Neurosci Lett*. 2010;480:69–72.
13. Marziani E, Pomati S, Ramolfo P, Cigada M, Giani A, Mariani C, et al. Evaluation of retinal nerve fiber layer and ganglion cell layer thickness in Alzheimer's disease using spectral-domain optical coherence tomography. *Invest Ophthalmol Vis Sci*. 2013;54:5953–8.
14. Paquet C, Boissonnot M, Roger F, Dighiero P, Gil R, Hugon J. Abnormal retinal thickness in patients with mild cognitive impairment and Alzheimer's disease. *Neurosci Lett*. 2007;420:97–9.
15. Iseri PK, Altinas O, Tokay T, Yuksel N. Relationship between cognitive impairment and retinal morphological and visual functional abnormalities in Alzheimer disease. *J Neuroophthalmol*. 2006;26:18–24.
16. Kesler A, Vakhapova V, Korczyn AD, Naftaliev E, Neudorfer M. Retinal thickness in patients with mild cognitive impairment and Alzheimer's disease. *Clin Neurol Neurosurg*.
17. Kromer R, Serbecic N, Hausner L, Froelich L, Aboul-Enein F, Beutelspacher SC. Detection of retinal nerve fiber layer defects in Alzheimer's disease using SD-OCT. *Front Psychiatry*. 2014;5:22.
18. Patton N, Aslam T, MacGillivray J, et al. Retinal vascular image analysis as a potential screening tool for cerebrovascular disease. *J Anat* 2005;206:318–48.
19. Bill, A. & Sperber, G. O. Control of Retinal and Choroidal Blood Flow. *Eye* 4, 1990;319–325.
20. Spaide RF, Klancnik JM, Cooney MJ, et al. Retinal vascular layers imaged by fluorescein angiography and optical coherence tomography angiography. *JAMA Ophthalmol* 2015;133:45.
21. Snodderly DM, Weinhaus RS, Choi JC. Neural-vascular relationships in central retina of macaque monkeys (*Macaca fascicularis*). *J Neurosci* 1992;12:1169–93.
22. Conrath J, Giorgi R, Raccach D, et al. Foveal avascular zone in diabetic retinopathy: quantitative vs qualitative assessment. *Eye* 2005;19:322–6.
23. Parodi MB, Visintin F, Della Rupe P, et al. Foveal avascular zone in macular branch retinal vein occlusion. *Int Ophthalmol* 1995;19:25–8.
24. Jian Y, Chunhui J, Xiaolei W, et al. Macula perfusion in healthy chinese—an optical coherence tomography angiogram study[J]. *Invest Ophthalmol Vis Sci* 2015;56(5):3212-3217
25. WANG X, KONG X, JIANG C, et al. Is the peripapillary retinal perfusion related to myopia in healthy eyes? A prospective comparative study[J]. *BMJ Open*, 2016, 6(3): e010791.
26. YANG Y, WANG J, JIANG H, et al. Retinal microvasculature alteration in high myopia[J]. *Invest Ophthalmol Vis Sci*, 2016, 57(14): 6020-6030
27. LI M, YANG Y, JIANG H, et al. Retinal microvascular network and microcirculation assessments in high myopia[J]. *Am J Ophthalmol*, 2017, 174: 56-67.
28. Spencer RJ, Wendell CR, Giggey PP, Katzel LI, Lefkowitz DM, Siegel EL, et al. Psychometric limitations of the Mini-mental State Examination among nondemented older adults: an evaluation of neurocognitive and magnetic resonance imaging correlates. *Exp Aging Res*. 2013;39(4):382–97.

29. Lonie JA, Tierney KM, Ebmeier KP. Screening for mild cognitive impairment: a systematic review. *Int J Geriatr Psychiatry*. 2009;24(9):902–15.
30. Beatty WW, Goodkin DE. Screening for cognitive impairment in multiple sclerosis. An evaluation of the Mini-Mental State Examination. *Arch Neurol*. 1990;47(3):297–301.
31. Swirsky-Sacchetti T, Field HL, Mitchell DR, Seward J, Lublin FD, Knobler RL, et al. The sensitivity of the Mini-Mental State Exam in the white matter dementia of multiple sclerosis. *J Clin Psychol*. 1992;48(6):779–86.
32. Moser DJ, Cohen RA, Clark MM, Aloia MS, Tate BA, Stefanik S, et al. Neuropsychological functioning among cardiac rehabilitation patients. *J Cardiopulm Rehabil*. 1999;19(2):91–7.
33. Tombaugh TN, McIntyre NJ. The Mini-Mental State Examination: A comprehensive review. *J Am Geriatr Soc*. 1992;40(9):922–35.
34. Nasreddine ZS, Phillips NA, Bedirian V, Charbonneau S, Whitehead V, Collin I, et al. The Montreal Cognitive Assessment, MoCA: a brief screening tool for mild cognitive impairment. *J Am Geriatr Soc*. 2005;53(4):695–9.
35. Luis CA, Keegan AP, Mullan M. Cross validation of the Montreal Cognitive Assessment in community dwelling older adults residing in the Southeastern US. *Int J Geriatr Psychiatry*. 2009;24(2):197–201.
36. Freitas S, Simões MR, Alves L, Santana I. Montreal Cognitive Assessment: validation study for mild cognitive impairment and Alzheimer disease. *Alzheimer Dis Assoc Disord*. 2013;27(1):37–43.
37. Roalf DR, Moberg PJ, Xie SX, Wolk DA, Moelter ST, Arnold SE. Comparative accuracies of two common screening instruments for classification of Alzheimer's disease, mild cognitive impairment, and healthy aging. *Alzheimers Dement*. 2013;9(5):529–37.
38. Ts'o MO, Bettman JW. Occlusion of choriocapillaris in primary nonfamilial amyloidosis. *Arch Ophthalmol* 1971;86:281–6
39. Roybal CN, Sanfilippo CJ, Nazari H, et al. Multimodal imaging of the retina and choroid in systemic amyloidosis. *Retin Cases Brief Rep* 2015;9:339–46
40. Gilmore GC, Levy JA. Spatial contrast sensitivity in Alzheimer's disease: a comparison of two methods. *Optom Vis Sci* 1991; 68: 790–794.
41. Nearing SA, Stone ER, Cronin-Golomb A, Oross S 3rd. The impact of acuity on performance of four clinical measures of contrast sensitivity in Alzheimer's disease. *J Gerontol B Psychol Sci Soc Sci* 2003; 58: P54–P62.
42. Cronin-Golomb A. Vision in Alzheimer's disease. *Gerontologist* 1995; 35: 370–376.
43. V Polo, MJ Rodrigo, E Garcia-Martin, et al. Visual dysfunction and its correlation with retinal changes in patients with Alzheimer's disease. *Eye*, 2017, 31, 1034–1041.
44. Robert A. Hao F. Retinal Oxygen: from animals to humans. *Prog Retin Eye Res*. 2017 May; 58: 115–151.
45. Carlisle R, Lanphier EH, Rahn H. Hyperbaric Oxygen and Persistence of Vision in Retinal Ischemia. *J Appl Physiol*. 1964;19:914–918.

46. Anderson B, Jr, Saltzman HA. Retinal Oxygen Utilization Measured by Hyperbaric Blackout. Arch Ophthalmol. 1964;72:792–795.
47. Polak K, Schmetterer L, Riva CE. Influence of flicker frequency on flicker-induced changes of retinal vessel diameter. Invest Ophthalmol Vis Sci. 2002;43:2721–2726.
48. Riva CE, Falsini B, Logean E. Flicker-evoked responses of human optic nerve head blood flow: luminance versus chromatic modulation. Invest Ophthalmol Vis Sci. 2001;42:756–762.
49. Falsini B, Riva CE, Logean E. Flicker-evoked changes in human optic nerve blood flow: relationship with retinal neural activity. Invest Ophthalmol Vis Sci. 2002;43:2309–2316.
50. Kotliar KE, Vilser W, Nagel E, Lanzl IM. Retinal vessel reaction in response to chromatic flickering light. Graefes Arch Clin Exp Ophthalmol. 2004;42:377–392.
51. Wang Y, Fawzi AA, Tan O, Zhang X, Huang D. Flicker-induced changes in retinal blood flow assessed by Doppler optical coherence tomography. Biomed Opt Express. 2011a;2:1852–1860.
52. Brown JS, Flitcroft DI, Ying GS, et al. In vivo human choroidal thickness measurements: evidence for diurnal fluctuations. Invest Ophthalmol Vis Sci. 2009; 50(1): 5-12.
53. Chakraborty R, Read SA, Collins MJ. Diurnal variations in axial length, choroidal thickness, intraocular pressure, and ocular biometrics. Invest Ophthalmol Vis Sci. 2011; 52(8): 5121-5129.
54. Tan CS, Ouyang Y, Ruiz H, et al. Diurnal variation of choroidal thickness in normal, healthy subjects measured by spectral domain optical coherence tomography. Invest Ophthalmol Vis Sci. 2012; 53(1): 261-266.

Tables

Table 1 Comparison of the basic clinical data between the ATD group and normal control group

	ATD group	Normal group	c ² or t
Sex [Male Female]	15/14	10/16	0.973
Eye [Right Left]	13/16	12/14	0.010
Age	68.38 ± 8.504	64.81 ± 6.462	1.738
IOP [mmHg]	14.24 ± 3.02	13.67 ± 2.39	0.767
CCT [μm]	539.62 ± 31.89	547.03 ± 36.09	-0.809
AL [mm]	23.90 ± 1.58	23.35 ± 0.82	1.644
MMSE score	24.90 ± 3.61	29.84 ± 0.37	-7.343
MoCA score	21.10 ± 3.97	29.46 ± 0.81	-11.090

ATD, Alzheimer's type dementia; AL, axial length; CCT, central corneal thickness; IOP, intraocular pressure; MMSE, Mini-Mental State Examination; MoCA, Montreal Cognitive Assessment.

Table 2 Comparison of vessel length density in different areas of the macula between the ATD group and normal group ($\bar{x}\pm s$, mm^{-1})

Location	Normal group(n=26)	ATD group (n=29)	t	P *
Foveolar subfield	6.43±3.14	3.78±2.84	3.289	0.002
The average vessel length density	16.08±1.94	14.20±2.77	2.902	0.005
The inner sector of the fovea				
Superior	16.63±2.15	13.40±3.90	3.849	0.000
Nasal	15.64±3.44	13.54±3.76	2.152	0.036
Inferior	16.34±2.30	13.51±3.79	3.383	0.001
Temporal	16.33±2.72	13.75±3.58	2.984	0.004
Average	16.18±2.23	13.55±3.27	3.520	0.001
The outer sector of the fovea				
Superior	16.44±2.41	14.53±3.23	2.461	0.017
Nasal	17.97±2.04	16.69±2.79	1.967	0.055
Inferior	16.45±1.66	14.54±3.43	2.672	0.011
Temporal	14.84±2.97	13.32±3.69	1.671	0.101
Average	16.41±1.92	14.77±2.74	2.554	0.014

The results are presented as the means \pm standard deviations of the original data.

* The independent sample t test was used to compare the difference in vessel length density between the ATD group and the normal group.

Table 3 Comparison of the **vessel width density** in different areas of the macula between the ATD group and normal control group ($\bar{x}\pm s$)

Location	Normal group_(n=26)	ATD group_(n=29)	t	P *
Foveolar subfield	0.159 \pm 0.12	0.080 \pm 0.06	3.115	0.003
The average vessel width density	0.392 \pm 0.05	0.343 \pm 0.07	2.885	0.006
The inner sector of the fovea				
Superior	0.397 \pm 0.05	0.314 \pm 0.10	3.982	0.000
Nasal	0.367 \pm 0.08	0.315 \pm 0.09	2.170	0.035
Inferior	0.391 \pm 0.06	0.318 \pm 0.09	3.502	0.001
Temporal	0.388 \pm 0.07	0.321 \pm 0.09	3.008	0.004
Average	0.386 \pm 0.06	0.317 \pm 0.08	3.674	0.001
The outer sector of the fovea				
Superior	0.404 \pm 0.06	0.358 \pm 0.09	2.248	0.029
Nasal	0.439 \pm 0.05	0.406 \pm 0.08	1.881	0.066
Inferior	0.408 \pm 0.08	0.358 \pm 0.09	2.636	0.012
Temporal	0.365 \pm 0.08	0.323 \pm 0.09	1.785	0.080
Average	0.403 \pm 0.05	0.361 \pm 0.07	2.511	0.015

The results are presented as the means \pm the standard deviations of the original data.

* The independent sample t test was used to compare the difference in vessel width density between the ATD group and the normal group.

Table 4 Univariate and multivariate regression analyses of the vessel parameters and ocular parameters of all subjects

	complete vessel length density	complete vessel width density	
	bb 95% confidence intervalP	bb 95% confidence intervalP	
Univariate regression analysis			
Age	-0.099(-0.187, -0.012)	0.027-0.002(-0.005, 0.000)	0.034
IOP (mmHg)	0.076 (-0.183, 0.335)	0.5580.002 (-0.004, 0.009)	0.480
AL (mm)	-0.599(-1.122, -0.077)	0.025-0.017(-0.031, -0.004)	0.013
CCT (µm)	-0.006(-0.027, 0.014)	0.5370.000 (-0.001, 0.000)	0.591
MMSE score	0.293 (0.114, 0.472)	0.0020.007 (0.003, 0.012)	0.002
MoCA score	0.194 (0.066, 0.322)	0.0040.005 (0.002, 0.008)	0.004
multivariate regression analysis			
Age	-0.654	0.104-1.550	0.127
AL (mm)	-0.527(-1.012, -0.043)	0.034-0.015(-0.028, -0.003)	0.016
MMSE score	0.275 (0.102, 0.449)	0.0020.007 (0.002, 0.011)	0.003
MoCA score	-0.101	0.920-0.063	0.950

ATD, Alzheimer’s type dementia; AL, axial length; CCT, central corneal thickness; IOP, intraocular pressure

Table 5 Univariate and multivariate regression analyses of the FAZ and eye parameters of all subjects

Table 6 Univariate and multivariate regression analyses of the average choroidal thickness and eye parameters of all subjects

Figures

FAZ

β 95% confidence interval P

Univariate regression analysis

Age	0.254 (0.008, 0.456)	0.062
IOP (mmHg)	0.197 (0.018, 0.379)	0.150
AL (mm)	-0.071(-0.293, 0.178)	0.607
CCT (μ m)	0.008 (-0.285, 0.317)	0.953
MMSE score	-0.342(-0.564, -0.135)	0.011
MoCA score	-0.451(-0.655, -0.261)	0.001

Multivariate regression analysis

MMSE score	0.429	0.158
MoCA score	-0.011(-0.017, 0.005)	0.001

average choroidal thickness (CT)

β 95% confidence interval P

Univariate regression analysis

Age	-0.803(-1.400, -0.206)	0.009
IOP (mmHg)	-0.991(-3.269, 1.287)	0.388
AL (mm)	-3.057(-7.675, 1.561)	0.190
CCT (mm)	-0.079(-0.256, 0.098)	0.953
MMSE score	5.638 (4.685, 6.592)	<0.001
MoCA score	4.053 (3.441, 4.666)	<0.001

Multivariate regression analysis

MMSE score	0.039	0.588
MoCA score	0.296	0.063

Univariate regression analysis	4.053 (3.441, 4.666)	<0.001
--------------------------------	----------------------	--------

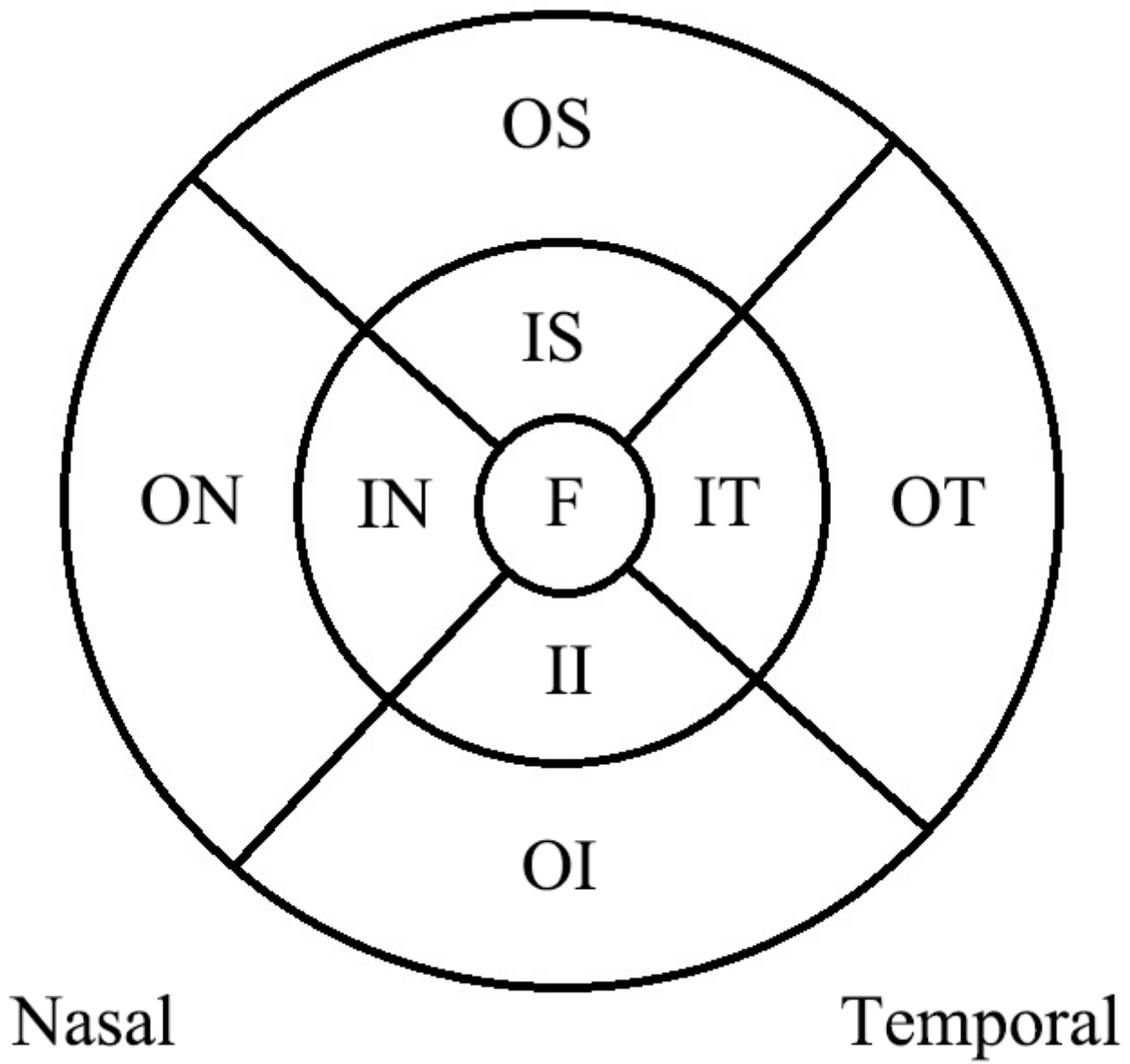


Figure 1

Schematic of 1, 3, and 6 mm ETDRS.

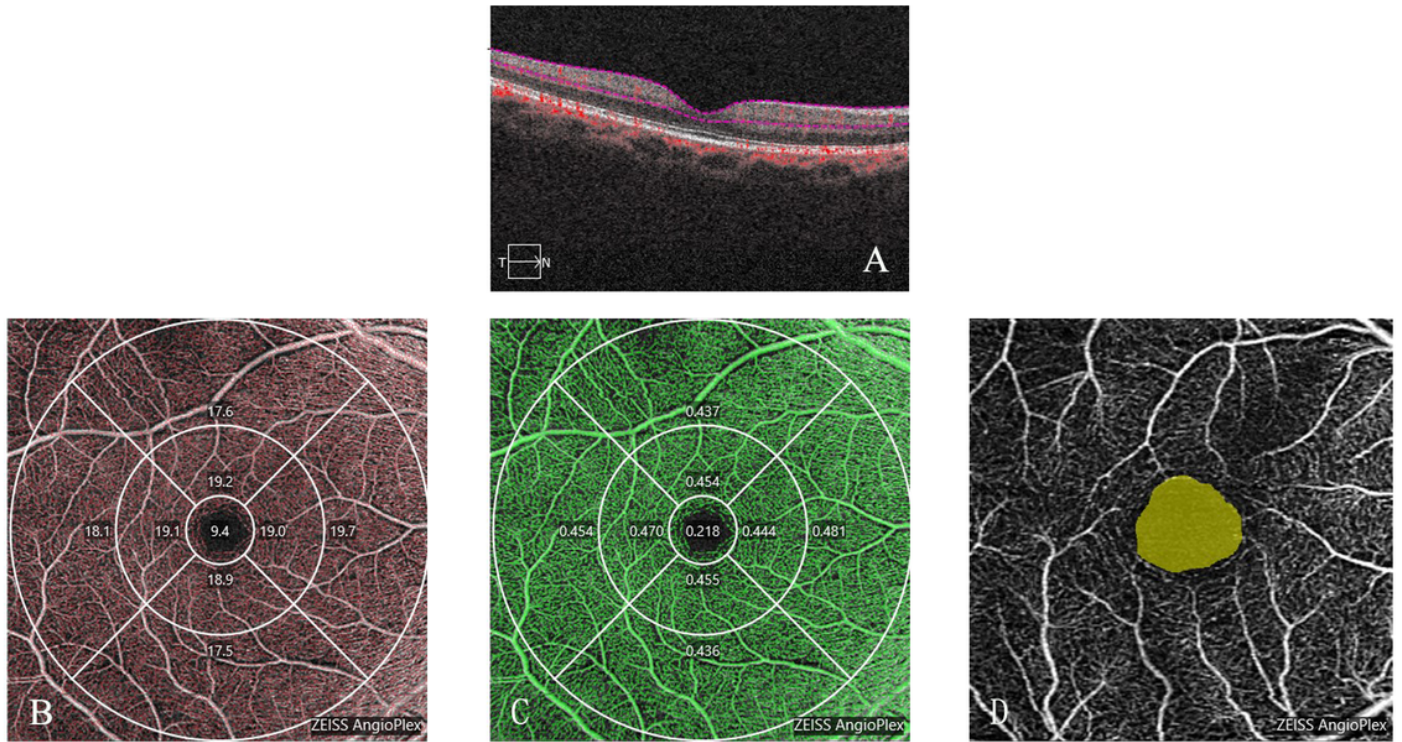


Figure 2

[A] Image of the surface retina blood flow signals from the internal limiting membrane (ILM) to the inner plexiform layer (IPL), which were used to analyse the overall vessel length density and vessel width density. [B] OCTA image overlaid on the schematic diagram showing the vessel length density image acquired in angiography 6×6 mm mode. [C] Image of the vessel width density acquired in angiography 6×6 mm mode. [D] FAZ area obtained using angiography 3×3 mm mode.

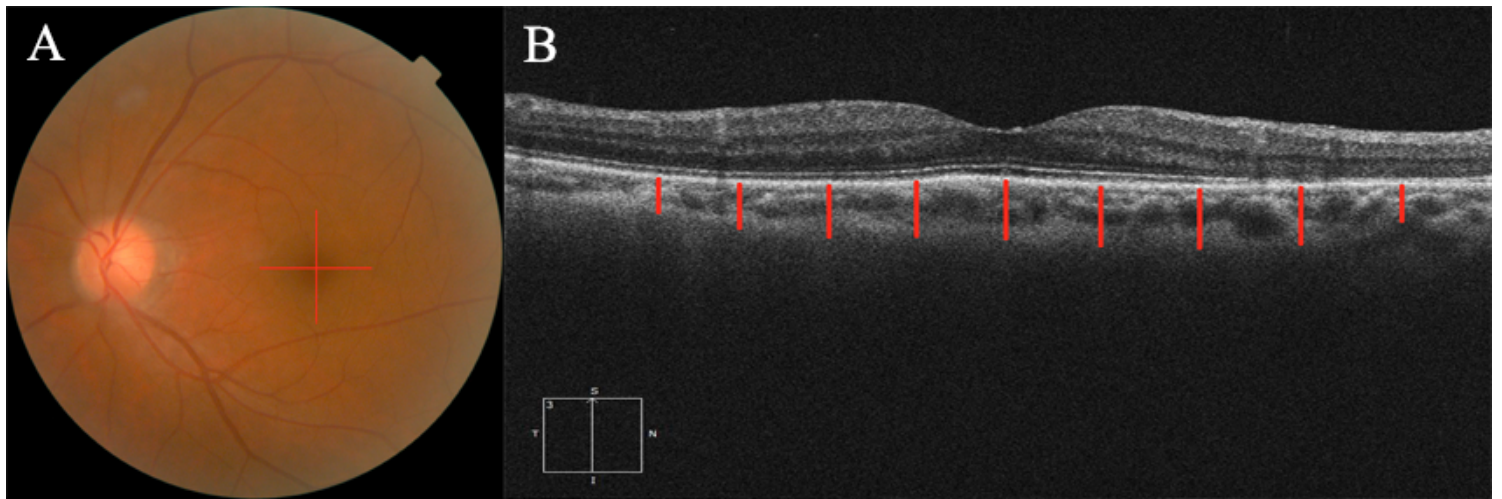


Figure 3

Schematic showing the measurement of the choroid thickness around the macular area using optical coherence tomography. (A) The positions of the horizontal and vertical scan lines in the macular area are

shown. (B) The location at which the choroidal thickness was measured in the macular area; each red line is separated by 500 μm .

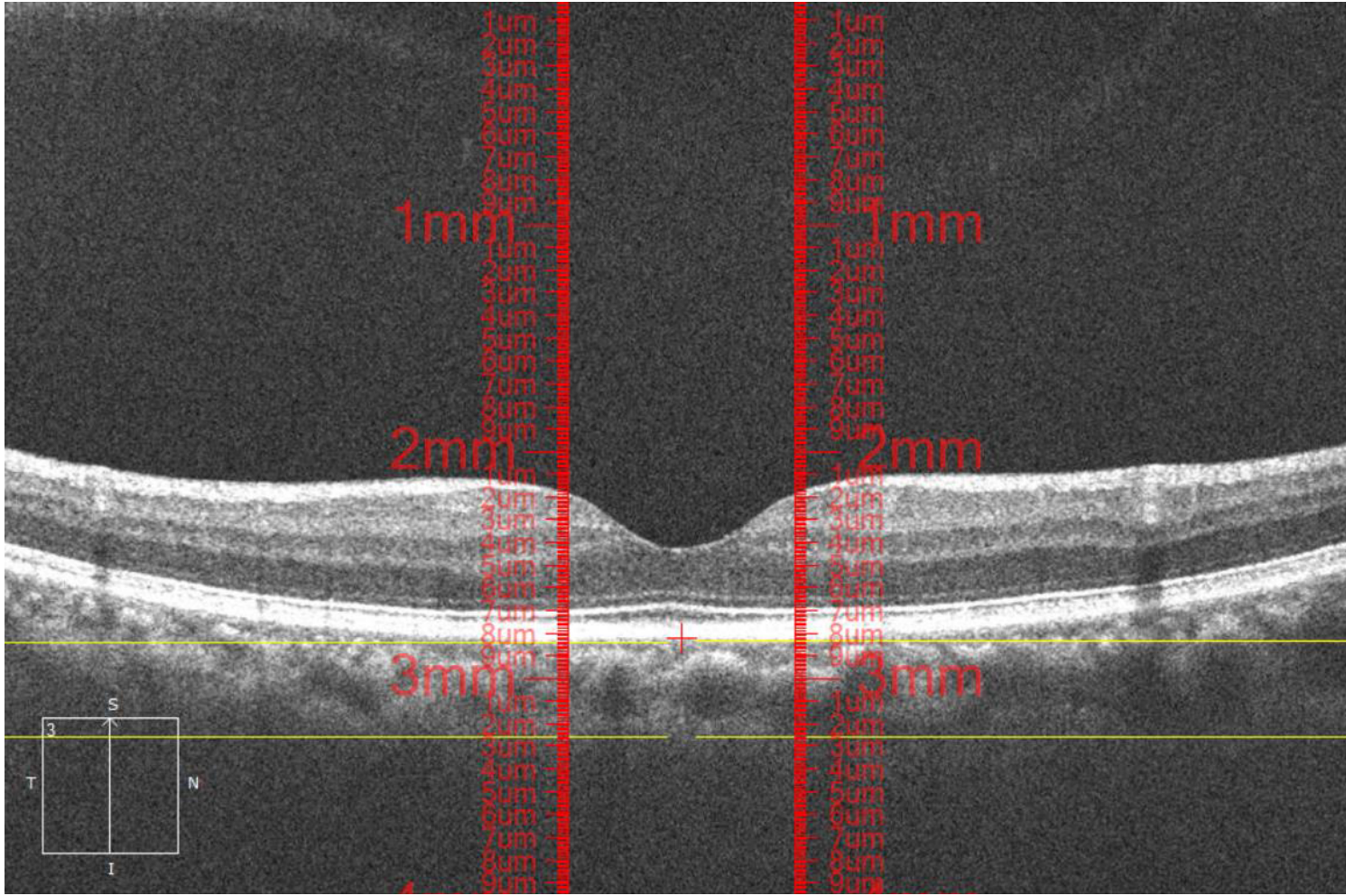


Figure 4

Interface diagram of the self-designed measurement software.

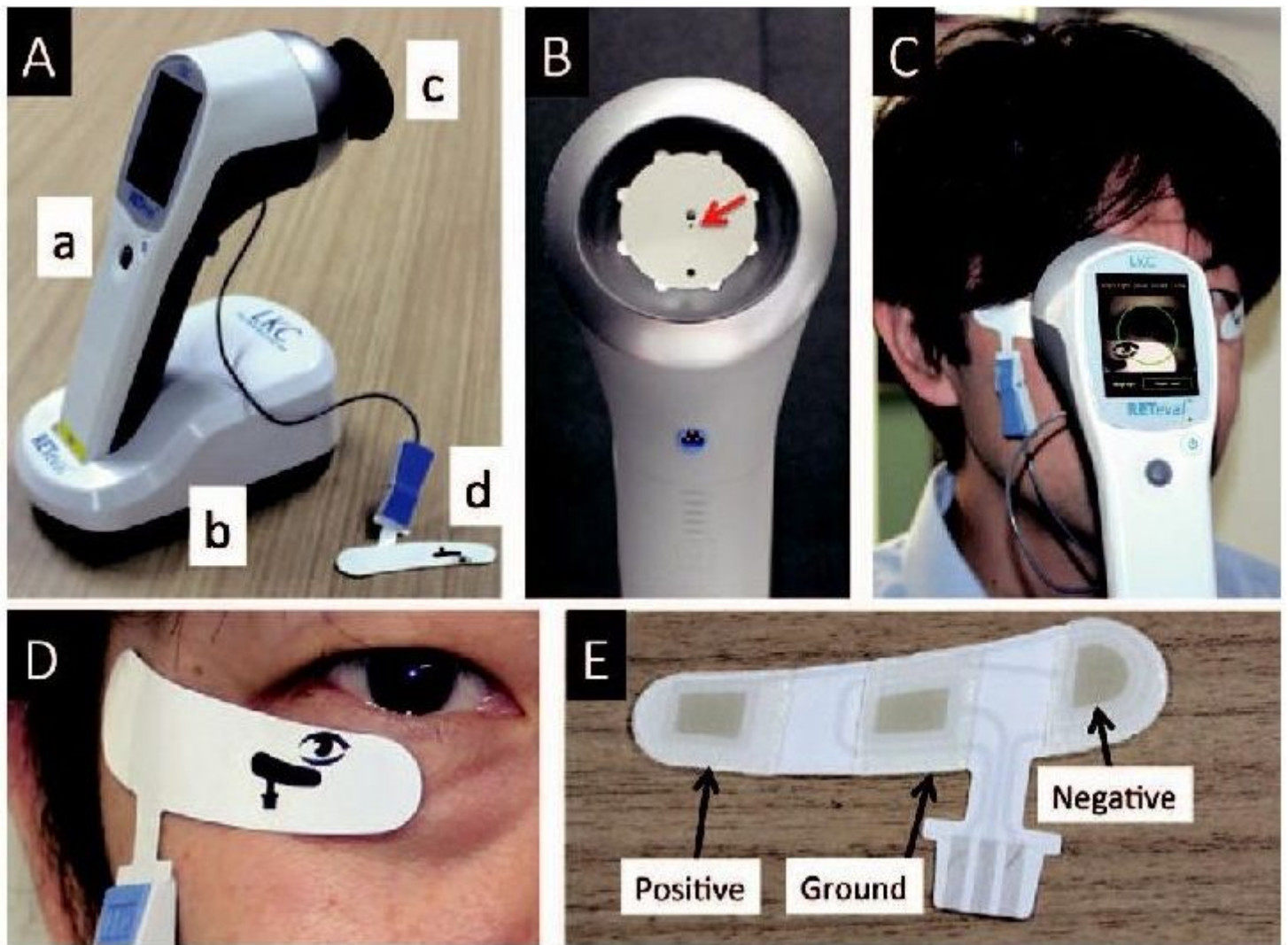


Figure 5

New handheld RETeval system. (A) The recording system consists of handheld stimulator, recording and analysis device (a), a joint base (b), a soft patch that contacts the bony area around the eyes (c) and a disposable skin electrode array (d). (B) The centre of the dome structure features a red fixation point (red arrows), and participants were asked to focus on that point during the ERG recording. (C) Acquisition process. (D) A skin electrode array (LKC Technologies, Inc.) was placed on the orbital margin 2 mm from the lower eyelid margin. (E) The electrode array comprises three electrodes, a positive electrode, a negative electrode and a ground electrode, each of which is covered with tape.

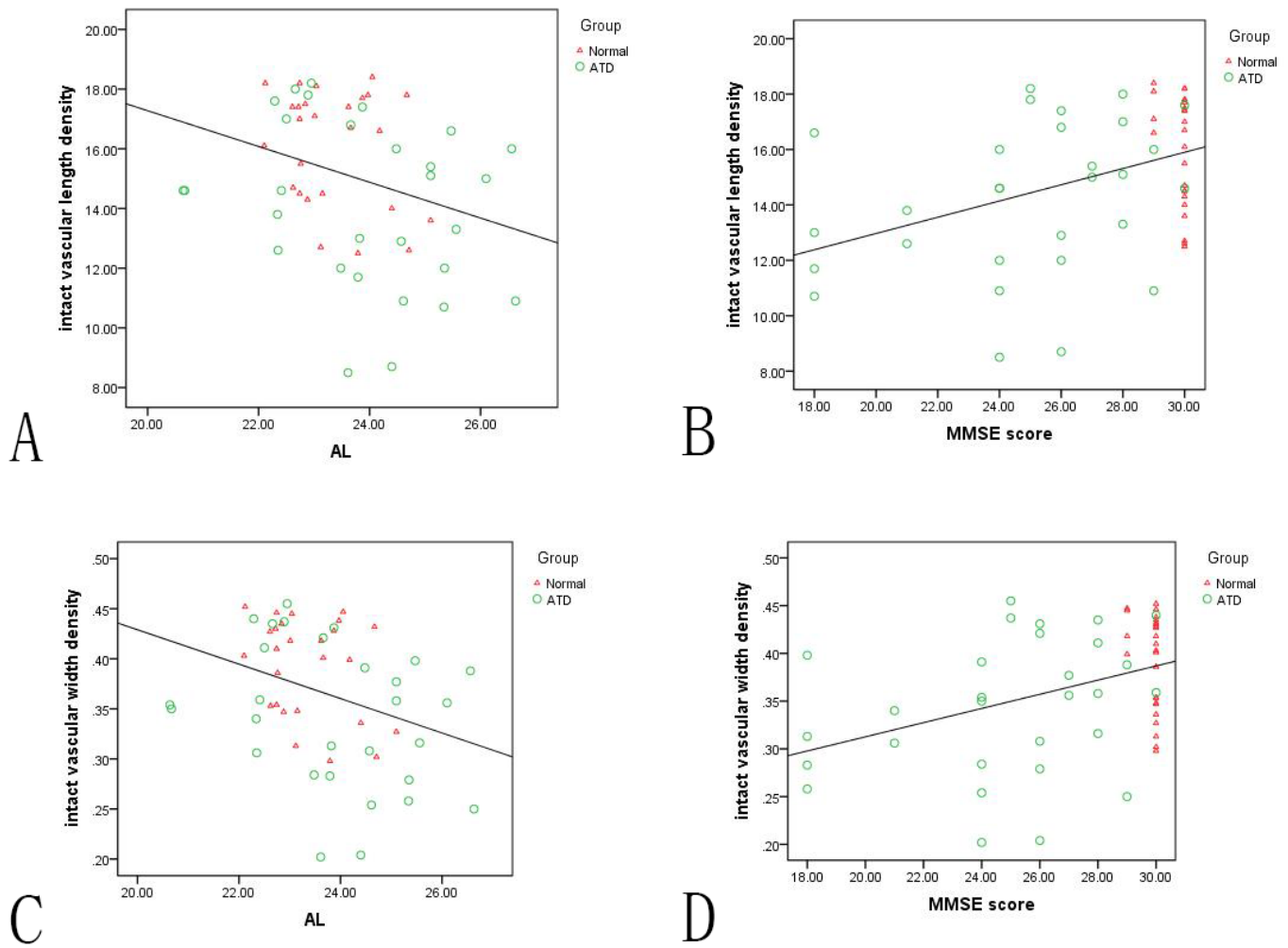


Figure 6

Scatter plots showing the correlations between the (A) complete vessel length density and axial length, (B) complete vessel length density and MMSE score, (C) complete vessel width density and axial length, and (D) complete vessel width density and MMSE score.

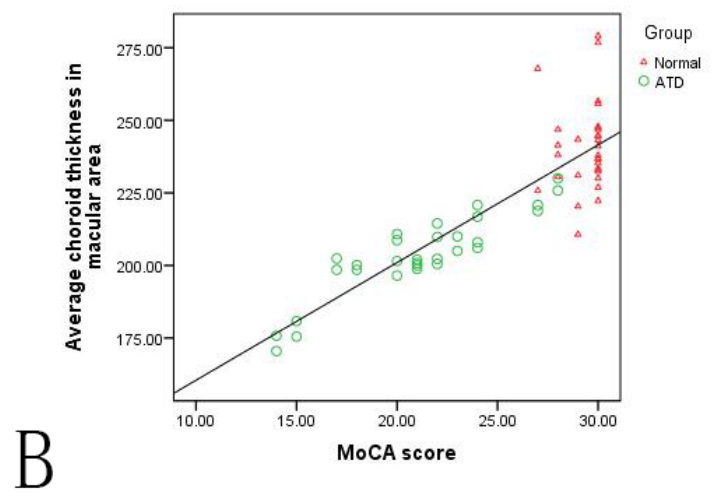
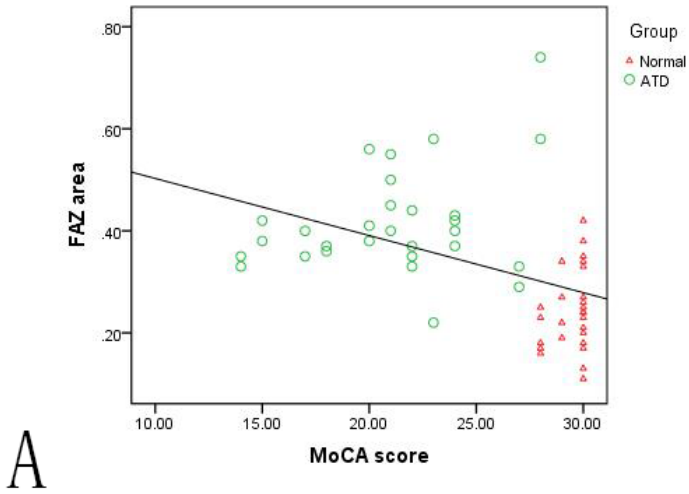


Figure 7

Scatter plot of the correlations between the (A) FAZ area and MoCA score and between (B) the CT and MoCA score.